Improving Wafer-Level Calibration Consistency with TMRR Calibration Method

Andrej Rumiantsev[1], Tony Fu[1], and Ralf Doerner[2]

[1]MPI Corporation, Advanced Semiconductor Test Division, Chu-Pei City, Taiwan
[2]Ferdinand-Braun-Institut (FBH), Leibniz-Institut fuer Hoechstfrequenztechnik, Berlin, Germany

Abstract — **This paper presents the new calibration algorithm TMRR (Thru-Match-Reflect-Reflect), the extension of the Thru-Match-Reflect (TMR) method with one extra Reflect standard. The algorithm was developed to reduce the impact of an asymmetrical placement of RF probes on coplanar probe-tip calibration standards on consistency and reproducibility of calibration results often observed for an inexperienced system operator. The introduction of an additional Reflect calibration element to the TMR algorithm increases the measurement information redundancy, and thus reduces the calibration error caused by possible asymmetry in reflection coefficients of lumped standards. The new method was verified for simulated data as well as for an InP DHBT device operating in the "off-state" regime.**

Index Terms — **S-parameters, calibration, on-wafer measurements.**

I. Introduction

The operation frequencies of semiconductor devices and circuits continuously increase and confront characterization engineers with new challenges: the device under test (DUT) pad de-embedding methods turn out to be complex and require additional dummy elements; the positioning of RF probe on calibration standards and DUT contact pads has to be more precise. It becomes hard to ensure accuracy, repeatability, and reproducibility of the system RF calibration and measurement data.

Implementing calibration standards into the device test chip significantly reduces back end of line (BEOL) parasitics, simplifies device parasitic de-embedding step and eliminates impact of the RF probe misplacement error on calibration standards [1]. However, is not always possible to scarify wafer real estate for custom calibration kits. Therefore, the alternative solution involves improving accuracy and consistency of the probe-tip calibration process conducted on commercially available alumina calibration substrates [2].

The calibration method of [3] enabled asymmetry of the Load equivalent impedance. As is was later demonstrated in [4], it is essential to measure Load standard on each VNA port during the calibration process. However, possible asymmetry in Reflect impedance (*e.g.* due to misplacement of RF probes on the standard) still remains the main contributing factor to the overall accuracy of the system calibration. This work extends the method of [4] by introducing additional Reflect standard to the conventional TMR calibration algorithm. The new TMRR method uses redundancy of standard measurements to reduce the impact of this type of error on accuracy and consistency of the system calibration.

The next chapter briefly describes the theoretical background of the TMRR calibration solution. The Chapter III presents verification results for the numerical experiment as well as for an active DUT.

II. Theoretical Background

The systematic measurement errors of a modern two-port double-reflectometer VNA can be fully described by the seven-term error model given by Fig. 1, where m_i denote the wave quantities measured by an ideal $i-$th VNA receiver; $[A]$ and $[B]$ are the 2x2 matrices of error terms; a_k and b_k are the wave quantities at the $k-$th port of the DUT, and $[T_X]$ is the T-parameter matrix of the DUT [5]. Self-calibration algorithms calculate $[A]$ and $[B]$ from measurement data of partly-known calibration standards, such as the Line and the Reflect for the TRL[1] method; reflect for the TMR, LRM[2].

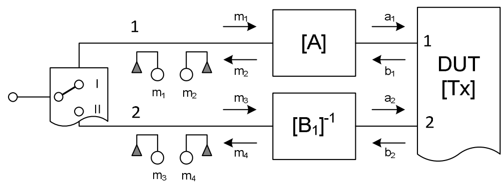

Fig. 1. The seven-term systematic error model of a two-port double reflectometer VNA.

Usually, the solution for the seven error terms consists of two steps: 1) calculation of the *a priori* unknown electrical characteristics of partly-known standards (*i.e.* "self-calibration step"); 2) calculation of the error terms based on the measured data of calibration standards and their now fully known electrical characteristics.

The relationship between the actual and measured T-parameters of a two-port DUT is given by:

$$[M_X] = [A][T_X][B]^{-1}, \qquad (1)$$

where $[M_X]$ is the measurement matrix:

[1] Thru-Reflect-Line
[2] Line-Reflect-Match

978-1-5386-5450-7/18/$31.00 ©2018 IEEE

$$[M_X] = \begin{bmatrix} m_1' & m_1'' \\ m_2' & m_2'' \end{bmatrix} \begin{bmatrix} m_3' & m_3'' \\ m_4' & m_4'' \end{bmatrix} = [m_a][m_b]^{-1}. \quad (2)$$

Prime and double-prime m_i denote data acquired in forward and reverse direction, respectively. The measurement of a one-port device with the reflection coefficient r_X on the first and the second VNA port yields Γ_{AX} and Γ_{BX}:

$$\Gamma_{AX} = \frac{m_1}{m_2} = \frac{A_{11}r_X + A_{12}}{A_{21}r_X + A_{22}}, \quad (3)$$

$$\Gamma_{BX} = \frac{m_3}{m_4} = \frac{B_{11} + B_{12}r_X}{B_{21} + B_{22}r_X}, \quad (4)$$

where :

$$r_X = \frac{b_1}{a_1} = \frac{b_2}{a_2}. \quad (5)$$

As shown in [5], the error-term matrixes $[A]$ and $[B]$ can be derived from measurements of at least three different standards: one fully known two-port element $[M_1]$ (e.g., Thru), one fully known element $[M_2]$ (e.g. Match, r_M), and one partly known $[M_3]$ one-port element (e.g. Reflect, r_R).

For the Thru standard, we have:

$$[T_1] = \begin{bmatrix} 1 & 0 \\ 0 & 1 \end{bmatrix}, \text{ and therefore: } [M_1] = [A][B]^{-1}. \quad (6)$$

Re-composing (2)-(4) and taking into account (6), we arrive at:

$$A_{11}r_{M1} + A_{12} - A_{21}r_{M1}\Gamma_{A1} - A_{22}\Gamma_{A1} = 0, \quad (7)$$
$$A_{11}r_{R1} + A_{12} - A_{21}r_{R1}\Gamma_{A2} - A_{22}\Gamma_{A2} = 0, \quad (8)$$
$$A_{11}c_1 + A_{12}r_{M2}c_1 - A_{21}c_2 - A_{22}r_{M2}c_2 = 0, \quad (9)$$
$$A_{11}c_3 + A_{12}r_{R2}c_3 - A_{21}c_4 - A_{22}r_{R2}c_4 = 0, \quad (10)$$

where Γ_{A1}, Γ_{B1} are measured results for the first r_M, and Γ_{A2}, Γ_{B2} for the second r_R one-port standard, respectively, with:

$$\begin{aligned} c_1 &= M_{1,22} + M_{1,21}\Gamma_{B1}, \\ c_2 &= M_{1,12} + M_{1,11}\Gamma_{B1}, \\ c_3 &= M_{1,22} + M_{1,21}\Gamma_{B2}, \\ c_4 &= M_{1,12} + M_{1,11}\Gamma_{B2}. \end{aligned} \quad (11)$$

Equations (7)-(10) can be solved for *a priory* unknown r_R and forcing $r_{R1} = r_{R2}$. Thus, the unknown reflection coefficient of the second one-port calibration standard can be found without calculating error terms.

It is important to note, (7)-(10) do not impose any specific requirements to the first one-port standard r_M. In the most general case, it can be realized as an asymmetrical element with known arbitrary impedance, *i.e.* it is allowed:

$$r_{M1} \neq r_{M2} \quad (12)$$

This is particularly beneficial for on-wafer calibration: the reactance of the on-chip match standard is usually different between its ports due to asymmetry in the via stack.

The measurement, self-calibration and calibration steps can be extended by adding the third partly-known one-port element r_{RR}. Its reflection coefficient can be found in the same way as r_R. Thus, the three-standard calibration solution TMR is expanded to the four-standard method TMRR with a higher grade of measurement information redundancy.

III. Experimental Results and Analysis

A. Worst-Case Scenario of CPW Standards Asymmetry

We conducted several experiments to verify the capability of the proposed calibration method. First, we defined the maximum possible asymmetry in equivalent impedances of lumped coplanar calibration standards. It is caused by misplacement of RF probes on the standard (Fig. 2). These errors usually occur in case of inexperienced system operators, entry-level manual wafer probe systems equipped with low-resolution microscopes, inaccurate or unstable chuck stages and imprecise RF probe positioners. For a paired symmetrical one-port standard, the maximum asymmetry of its equivalent impedance corresponds to the maximal lateral shift of both RF probes either to the left or to the right [6]. So, one probe entirely overlaps the standard contact pad while the other probe barely touches the edge of the pad (Fig. 3).

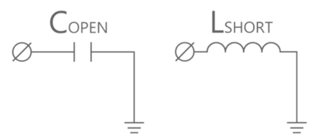

a) b) c)

Fig. 2. Equivalent impedance models of lumped standards: a) Load, b) Open, c) Short

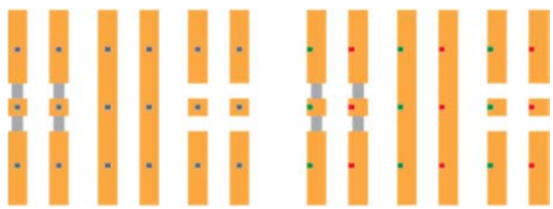

a) b)

Fig. 3. From left to right: probe-tip coplanar Load, Open, and Short standards in ground-signal-ground (GSG) configuration with central RF probe contact points, *i.e.* nominal equivalent impedance, a), and same standards contacted with maximal lateral shift of RF probes to the left, *i.e.* maximum asymmetry of the standard equivalent impedance, b).

In this experiment, we used an AC2 calibration substrate from MPI Corporation that includes Open, Short, Load, Thru and five calibration Lines in CPW design. It can be used for calibrating RF probes in GSG configuration of pitches from 100 µm to 250 µm. The lumped standard width is 50 µm and thus, the maximal possible lateral shift of RF probes is 25 µm. Table I presents the nominal equivalent model parameters of calibration standards as well as the extracted model parameters for the shifted configuration of the probes.

Because the probe-to-probe distance remained unchanged, we did not observe any variations in extracted model parameters for the thru standard.

TABLE I
EXTRACTED MODEL PARAMETERS OF EQUIVALENT IMPEDANCE OF CPW STANDARDS USED IN THE EXPERIMENT

Standard	Nominal		Shifted	
	P1	P2	P1	P2
Open, fF	5.8	5.8	5.1	6.5
Load, pH	-6.0	-6.0	0.5	-11.7
Short, pH	0.8	0.8	6.5	-5.0

Our experiment focused on the worst-case scenario with off-wafer standards (located directly under the probe tips) and the maximum lateral shift of the probes. In this case we have the highest asymmetry between standard impedances. On-wafer calibration standards, however, are located relatively far from the probe tips. Thus, they are significantly less sensitive to the RF probe placement error.

B. Evaluation of Calibration Error Caused by Standards Asymmetry

Next, we evaluated the measurement error of the verification devices caused by the maximum positioning error of RF probes on lumped CPW standards during system calibration. This experiment used synthesized raw data series of calibration standards and verification elements, DUT-PAD-OPEN and DUT-PAD-SHORT, respectively. The DUT-PAD-OPEN is a capacitor of C_O=270 fF and the DUT-PAD-SHORT is a series connection of a resistor R_S=3 Ω and an inductor L_S=20 pH. Similar elements are commonly used as dummy structures for de-embedding of the back end of line parasitics of silicon processes (Fig. 4).

We modeled two sets of calibration standard raw *S*-parameters: the "reference set" – using nominal standard model coefficients, and the "shifted set" – representing the worst-case probe positioning error on all lumped-element standards (Fig. 2-3, Table I). Next, we executed three calibrations series and respectively corrected verification DUTs: TMR with Short as the Reflect (TMR(S)), TMR with the Open as the Reflect (TMR(O)), and TMRR, with the same Short standard as the first Reflect and the Open as the second Reflect element. Fig. 5-6 show the experimental results.

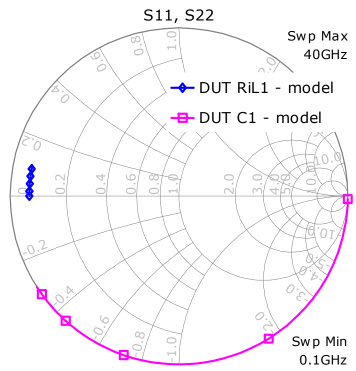

Fig. 4. *S*-parameters of the verification DUT-PAD-SHORT and DUT-PAD-OPEN devices.

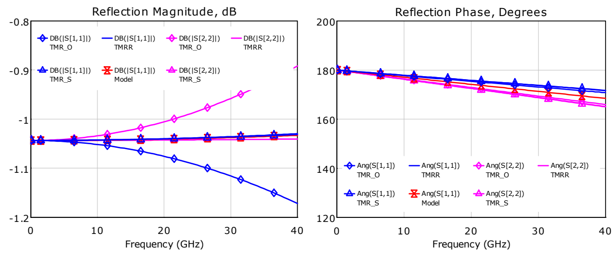

Fig. 5. S_{11} and S_{22} of the DUT_PAD_SHORT device corrected with the respect to TMR(O), TMR(S) and TMRR methods.

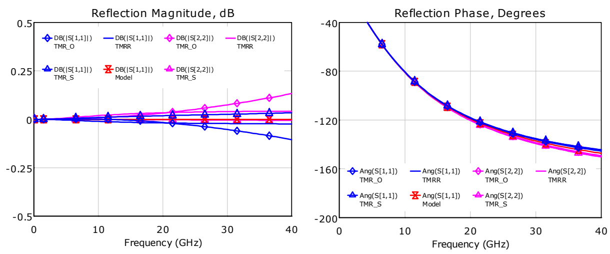

Fig. 6. S_{11} and S_{22} of the DUT_PAD_OPEN device corrected with respect to TMR(O), TMR(S) and TMRR methods.

This experiment demonstrated that the asymmetry error in lumped standards affects the accuracy of all evaluated methods. However, if only one reflect element (Open or Short) is used for calibration, the measurement error becomes dominant at the opposite site of the Smith chart. For instance, error is less for the DUT-PAD-SHORT element for TMR(S), while TMR(O) shows the largest error for this device. For the same data set, the TMRR error is significantly smaller for both devices. Also, the measurement error is dominant for the magnitude of the reflection coefficient of the verification DUTs. One the other hand, it is negligible for the phase.

Also, we observed a larger calibration error for the TMR(O) than for the TMR(S). While this effect requires further detailed analysis, we anticipate that it may be related to similarities in design of the probe tip Load and Short standards.

C. Verification for an Active DUT

Finally, we verified the new TMRR method by evaluating an HBT device. The HBT was fabricated in InP DHBT transferred-substrate technology from FBH. The off-wafer TMRR corrected measurements using a commercial calibration substrate were compared with the multiline TRL (mTRL) as well as the TMR method.

Accurate model parameter extraction is a crucial task for successful circuit design. We found, that special bias point measurements, which enable the extraction of certain important model parameters of an HBT [7], are extremely sensitive to the system calibration.

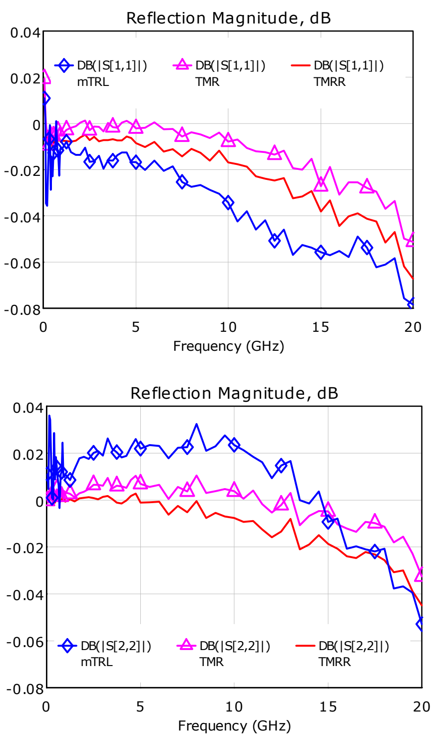

Fig. 7. Measurement results of an active DUT corrected with respect to off-wafer TMRR, multiline TRL, and TMR(S) calibration methods: S_{11} (top) and S_{22} (bottom).

The transistor reflection coefficient S_{22} (Fig. 7) that was measured in a so-called "off-state" bias point, exceeds one for both mTRL and TMR calibration methods (greater than 0 dB). Dealing with such data is very challenging for a modeling engineer. Fig. 7 demonstrates that the new TMRR method provides the most trustable measurement results for the test HBT under considered bias conditions. This ensures that the extraction of model parameters yields reasonable and reliable results.

IV. Conclusion

In this paper we introduced and verified the new calibration algorithm TMRR. This method extends the TMR procedure by an additional symmetrical Reflect element. The extra measurement step increases the information redundancy and thus reduces the calibration error caused by possible asymmetry in reflection coefficients of lumped standards. Such asymmetry is usually observed for probe-tip calibration on commercially available alumina coplanar standards.

Experimental results demonstrated that TMRR outperforms conventional methods that use only one Reflect standard. The new method is a good candidate for both probe tip and on-wafer system calibration.

References

[1] A. Rumiantsev, "On-Wafer calibration techniques enabling accurate characterization of high-performance silicon devices at the mm-wave range and beyond," Fakultät für Maschinenbau, Elektrotechnik und Wirtschaftsingenieurwesen, BTU Cottbus, Cottbus, 2014.

[2] A. Rumiantsev, P. Sakalas, N. Derrier, et al., "Influence of probe tip calibration on measurement accuracy of small-signal parameters of advanced BiCMOS HBTs," in IEEE Bipolar/BiCMOS Circuits and Technology Meeting (BCTM), Atlanta, GA, 2011.

[3] R. F. Scholz, F. Korndorfer, B. Senapati, et al., "Advanced technique for broadband on-wafer RF device characterization," in ARFTG Microwave Measurements Conference-Spring, 63rd, 2004, pp. 83-90.

[4] R. Doerner, "Evaluation of wafer-level LRRM and LRM+ calibration techniques," in ARFTG Microwave Measurements Conference-Spring, 69th, 2007, pp. 86-89.

[5] H. J. Eul and B. Schiek, "A generalized theory and new calibration procedures for network analyzer self-calibration," Microwave Theory and Techniques, IEEE Transactions on, vol. 39, pp. 724-731, 1991.

[6] A. M. E. Safwat and L. Hayden, "Sensitivity analysis of calibration standards for fixed probe spacing on-wafer calibration techniques," in Microwave Symposium Digest, 2002 IEEE MTT-S International, 2002, pp. 2257-2260.

[7] M. Rudolph, Introduction to Modeling HBTs. Boston, MA: Artech House, 2006.